

## DIAGNOSIS OF ARTICULAR CARTILAGE DAMAGE BY POLARIZATION SENSITIVE OPTICAL COHERENCE TOMOGRAPHY AND THE EXTRACTED OPTICAL PROPERTIES

**J.-J. Shyu**

Department of Veterinary Medicine  
National Taiwan University  
Taipei 106, Taiwan

**C.-H. Chan, M.-W. Hsiung, P.-N. Yang, H.-W. Chen  
and W.-C. Kuo**

Institute of Electro-optical Science and Technology  
National Taiwan Normal University  
88, Sec. 4, Ting-Chou Road, Taipei 116, Taiwan

**Abstract**—This paper presents a diagnosis method for articular cartilage damage using polarization-sensitive optical coherence tomography (PS-OCT). Through signal analysis, the optical characteristics of intact cartilage and different types of mild lesions within cartilages can be quantified from measures such as the scattering coefficient ( $\mu_s$ ), effective anisotropy factor ( $g_{eff}$ ), and birefringence coefficient ( $\Delta n$ ). Our preliminary investigation using porcine articular cartilage indicated that both subsurface morphological changes and apparent variations in optical properties, which may be the early signs of cartilage degeneration, were found in three types of diseased cartilages.

### 1. INTRODUCTION

Studies on articular cartilage are motivated by its critical role in the development of osteoarthritis (OA), a common cause of physical disability. Therefore, any sensitive technique for detecting the early signs of OA in cartilage would be valuable for monitoring disease progression and evaluating treatment efficacy. Various techniques have been developed for early and nondestructive diagnosis of cartilage

---

Corresponding author: W.-C. Kuo (kwchuan@ntnu.edu.tw).

disease [1]. The most widely used method for the assessment of joint disorders is arthroscopy, which cannot diagnose subsurface lesions. Others, including traditional radiography, computed tomography, magnetic resonance imaging, and conventional and high-frequency ultrasound, either lack the resolution or are not cost effective, thus limiting their widespread clinical use.

Optical coherence tomography (OCT), introduced in 1991, is a powerful tool for noncontact and noninvasive tomographic imaging of biological tissues [2]. OCT images are created from measurement of the echo time delay and intensity of backscattered light from a specimen. OCT employs the inherent differences in the index of refraction, rather than enhancement with dyes, to differentiate tissue types. It can achieve very high resolutions and has, for example, been successfully used for micron-scale imaging of osteoarthritic cartilage and progressive articular cartilage degeneration [3–5]. Besides, an arthroscopic microscopy of articular cartilage using OCT has also been proposed [6]. Polarization-sensitive OCT (PS-OCT), a type of functional OCT, combines the advantages of OCT with the additional image contrast obtained by using the birefringence characteristics of a specimen as a contrast agent [7]. It has been reported to be a potentially valuable diagnostic tool for the characterization of the collagen structure in human and equine joints and to determine the orientation of collagen fibers in articular cartilage and the meniscus [8–10].

As new treatments arise, there is an increased need for quantitative grading and accurate assessing damaged articular cartilage to measure treatment effects. Therefore, the use of PS-OCT for quantitative evaluation of optical properties in porcine articular cartilage was proposed in this study. We extracted the scattering coefficient ( $\mu_s$ ) and effective anisotropy factor ( $g_{eff}$ ) from PS-OCT intensity images (the same as OCT image). The birefringence coefficient ( $\Delta n$ ) was defined as being equal to the slope of the phase retardation versus distance. These optical properties were defined, quantified, and analyzed for intact and mildly damaged articular cartilages.

## 2. MATERIALS AND METHODS

Porcine joints with intact and mildly damaged cartilages (as determined by visual inspection) were obtained from a local abattoir that operated in accordance with relevant legislation. The PS-OCT setup used in this study has been described in detail previously [11]. Briefly, a collimated beam from a superluminescent diode (SLD) with a

central wavelength of 837 nm and a spectral bandwidth of 17.5 nm was used as a low-coherence light source in a Michelson interferometer. The axial resolution (which depends on the temporal coherence properties of the SLD) was 17  $\mu\text{m}$ , while the lateral resolution (determined by the numerical aperture of the objective) was 10  $\mu\text{m}$ . The specimens were mounted in a cuvette and moistened with normal saline bath maintained at 37°C during imaging. Each joint specimen was re-oriented for each measurement site so as to keep the incident light beam perpendicular to the articular surface. Fig. 1(a) shows the sample arm geometry used to generate two images (reflected intensity  $R$  and phase retardation  $\Phi$  as shown in Fig. 1(b)) simultaneously on the basis of the amplitude of the interference signal. An extended Huygens-Fresnel model [12], which is valid in both the single- and multiple-scattering regimes, was used to extract the optical scattering properties from

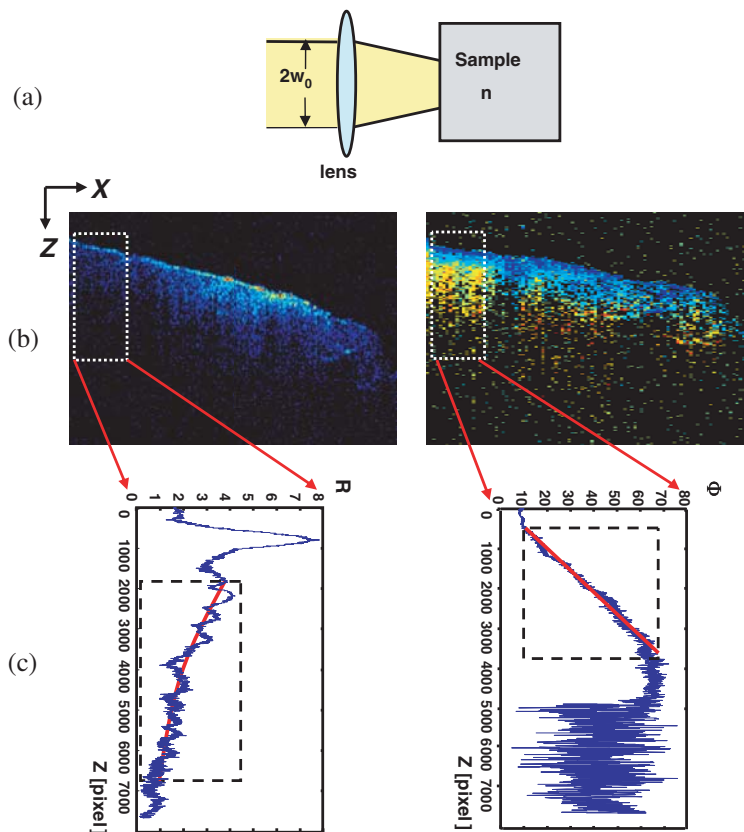


Figure 1. PS-OCT extraction algorithm.

the  $R$  image. First, images were automatically divided into several regions of interest (ROIs), e.g., the white dashed box in the left part of Fig. 1(b), spanning the joint surface and including approximately 25 lateral scans. After laterally (i.e., along the  $x$ -axis) delineating and averaging the  $R$  signals within each ROI, the  $\mu_s$  and root-mean-square scattering angle ( $\theta_{rms}$ ), which can be used to calculate the effective anisotropy factor ( $g_{eff} = \cos(\theta_{rms})$ ), were extracted by fitting the reflectivity signals as functions of depth to the extended Huygens-Fresnel model, as represented in the left part of Fig. 1(c). Then, the birefringence coefficient ( $\Delta n$ ) was determined by calculating the slope of the  $\Phi$  signal versus distance as represented in the right part of Fig. 1(c).

Following PS-OCT imaging and quantitative optical property extraction, all the specimens were subjected to decalcification for 3 days, then fixed in 10% neutral formalin for 24 hours, and finally processed for standard paraffin embedding. Serial sections with a thickness of 4  $\mu\text{m}$  were cut within the region of PS-OCT examination. Picrosirius red staining plus polarization microscopy were used to assess the collagen fiber structure in the cartilage. Specimens were then classified into “intact surface”, “mild damaged surface”, “fibrillation”, and “raised surface” cartilage by a pathologist (J. J. Shyu).

### 3. RESULTS

The PS-OCT images and corresponding histology of the visually healthy and damaged articular cartilages are shown in Figs. 2–5. Fig. 2(a) is a PS-OCT structural image showing a smooth surface and uniform reflectivity signals. In Fig. 2(b), the pseudo color representing the  $\Phi$  signal which shows that visually healthy cartilage has little birefringence when the incident light scans the tissue normal to the surface. The histological image (Fig. 2(c)) shows the collagen matrix in healthy cartilage arranged in three distinct morphological zones: the superficial zone (SZ), where collagen is parallel to the surface; the transitional zone (TZ), where collagen is transitional; and the radial zone (RZ), where collagen is perpendicular to the surface. With polarization microscopy (Fig. 2(d)), the bright regions stained with picrosirius were revealed, thick collagen fibers appeared yellowish-orange in color on the surface, and the thin collagen fibers appeared more greenish in the deeper regions.

Figure 3 presents an articular specimen with a mild damaged surface. The PS-OCT image in Fig. 3(a) shows a heterogeneous structure with subsurface defects (white arrowheads), which are confirmed by the corresponding histology in Fig. 3(c) (black

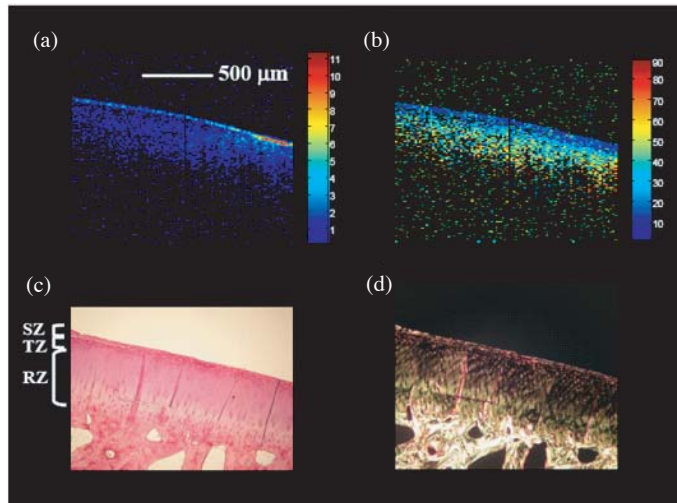


**Figure 2.** PS-OCT and the corresponding histological images of visually healthy cartilage. (a) Backscatter reflectivity image, (b) phase retardation image (linear color scale degrees), (c) histology (picrosirius red staining), and (d) picrosirius red staining plus polarization microscopy. SZ: superficial zone, TZ: transitional zone, RZ: radial zone.

arrowheads). Strong birefringence is found on right part of Fig. 3(b) due to cartilage thickening, while cartilage thinning is seen as a loss of polarization sensitivity on the left part of the image; both features were confirmed histologically as shown in Fig. 3(d).

The PS-OCT image in Fig. 4(a) shows fine fibrillations (white arrowheads) along with a partial-thickness tissue fissure (white arrow). While the specimen shows strong birefringence in the retardation image (Fig. 4(b)), it is not as homogeneous as in the tissue seen in the right part of Fig. 3(b) (i.e., collagen thickening). Histology confirmed deep fissures (black arrow) and superficial fibrillation (black arrow). Polarization microscopy revealed an increase in the full thickness of the cartilage, especially in the thick collagen fiber layer (with a yellowish-orange color).

A cartilage with a raised surface is shown in Fig. 5. The bright features in the reflectivity images (Fig. 5(a)) correspond to regions with a high density of optical scatterers. The retardation image (Fig. 5(b)) shows a stronger birefringence characteristic in the lateral cartilage (L) than in the medial region (M). New bone growth, which

is marked by \*, is revealed in Fig. 5(c). A comparison of Fig. 5(b) with Fig. 5(d) shows that the intense birefringence characteristic is due to cartilage thickening, apparently existed in the lateral cartilage region. Finally, PS-OCT images were subdivided into 40 ROIs (10 with fibrillation lesion) from the above articular specimens, the distribution of extracted data,  $\mu_s$ ,  $g_{eff}$ , and  $\Delta n$ , in 40 ROIs are shown in Fig. 6.

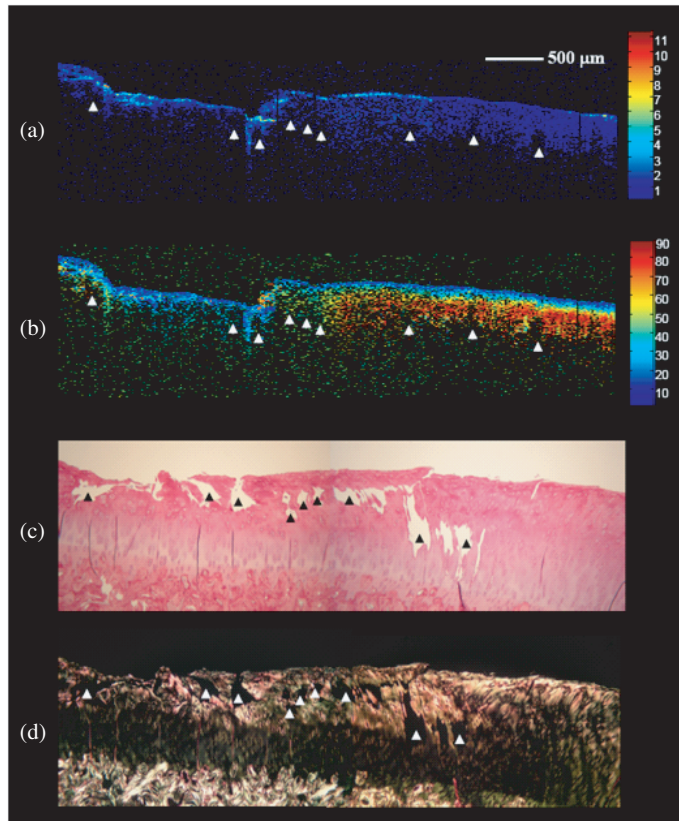


**Figure 3.** PS-OCT and corresponding histological images of cartilage with mild damaged surface. (a) Backscatter reflectivity image, (b) phase retardation image (linear color scale degrees), (c) histology (picrosirius red staining), and (d) picrosirius red staining plus polarization microscopy. Areas of defect are indicated by arrowheads.

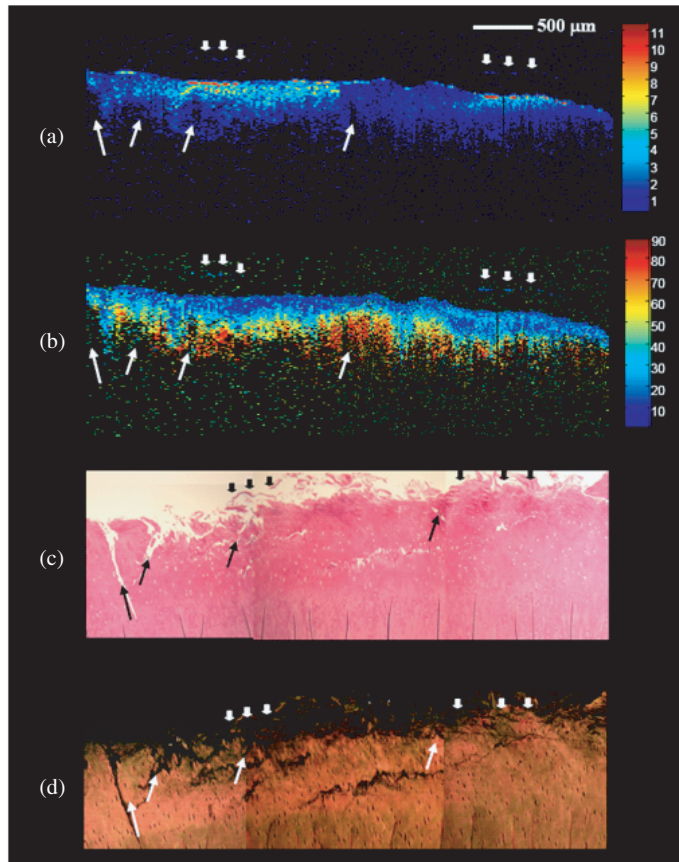


**Figure 4.** PS-OCT and corresponding histological images of cartilage with fibrillation. (a) Backscatter reflectivity image, (b) phase retardation image (linear color scale degrees), (c) histology (picosirius red staining), and (d) picosirius red staining plus polarization microscopy. Areas of fine fibrillation and fissure are indicated by arrowheads and arrows, respectively.

#### 4. DISCUSSION

In this study, the weightbearing regions of the porcine joint specimens were adopted because their pathogenesis of degeneration is similar to progressive articular cartilage degeneration in human. Mildly structural changes, including fine fibrillations, subsurface defects and fissures, were detected by PS-OCT and were confirmed by histology. The PS-OCT images and histopathology results both demonstrated

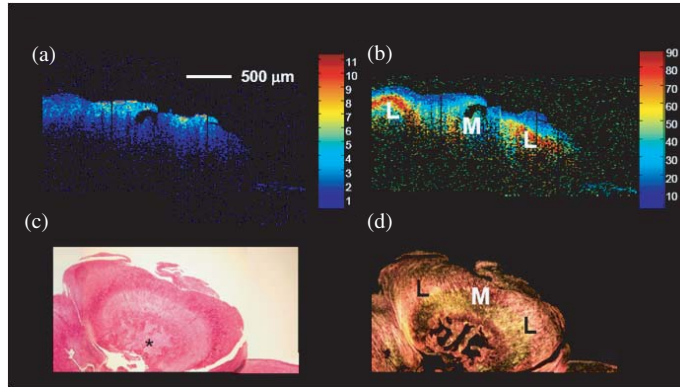


**Figure 5.** PS-OCT and corresponding histological images of cartilage with visually raised surface. (a) Backscatter reflectivity image, (b) phase retardation image (linear color scale degrees), (c) histology (picrosirius red staining), and (d) picrosirius red staining plus polarization microscopy. Areas of new bone growth are indicated by \*. L: lateral, M: medial region.

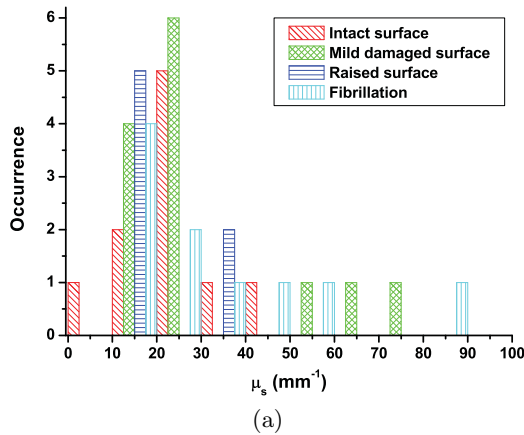
similar features that allowed the differentiation of normal cartilage from cartilage with lesions. The picrosirius-polarization method also confirmed the PS-OCT measurements of the presence or absence of organized collagen in the articular cartilage.

We also assess the condition of a cartilage lesion from quantitative optical properties extracted from both the scattering (i.e.,  $\mu_s$  and  $g_{eff}$ ) and birefringence (i.e.,  $\Delta n$ ) characteristics of articular specimens. The  $\mu_s$  can be thought of as the reciprocal of the average distance a photon travels between scattering events. The  $g_{eff}$  factor describes how isotropic or anisotropic the scattering is, and is related to the particle size in the specimen. The  $\Delta n$  value characterizes the differential speed of propagation between two orthogonal polarized states of light in the specimen; it may change with derangement and mechanical failure of the collagen network in the cartilage.

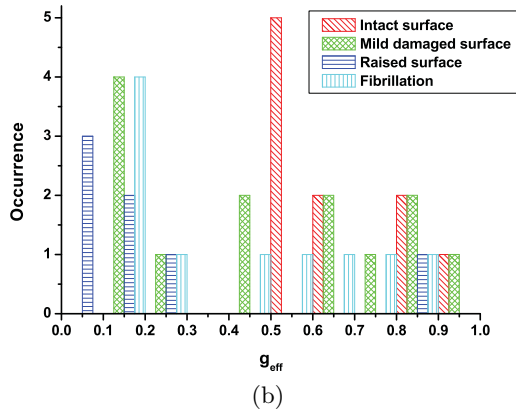
A uniform distribution of the scattering property was observed on visually intact cartilages, while spatial variations were found in the intrinsic low birefringence. The interpretation of this is that when the imaging light is directed normal to the cartilage surface,  $\Phi$  increases with depth only in the SZ. Minimal to no retardation is expected in the TZ and RZ, which is because the incident beam travels parallel to the orientation of the collagen fiber. In addition, the direction of individual collagen fiber in layered planes parallel to the surface may vary from

that of each other within a joint [18]. This induces a heterogeneous distribution of  $\Phi$  signals.

Almost all the normal cartilage and cartilage with raised surface lesion ROIs had  $\mu_s$  below  $40 \text{ mm}^{-1}$ , while cartilage with mild damaged surface and fibrillation lesions demonstrated considerable variations between  $10\sim 90 \text{ mm}^{-1}$  in  $\mu_s$  (Fig. 6(a)). The average  $\mu_s$  in cartilage with fine fibrillations is  $38.1 \pm 14.39 \text{ mm}^{-1}$ , which is the largest deviation from that in the intact articular tissue. This may originate from the fact that the fiber organization is disrupted in this kind of lesion. All of the normal cartilage samples had  $g_{eff}$  between 0.5 and 1, while  $g_{eff}$  was below 0.5 in approximately 54% of cartilage with mild damaged surface, 60% of cartilage with fibrillation, and 86% of cartilage with raised surface (Fig. 6(b)). The small value of  $g_{eff}$  existed most in cartilage with a raised surface may be due to the surface morphological changes. Approximately 80% of  $\Delta n$  values in



(a)



(b)

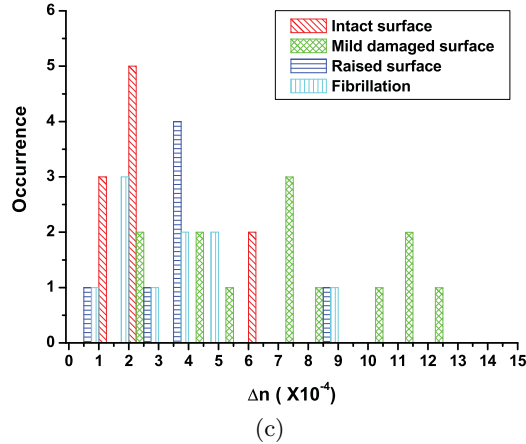


**Figure 6.** Distributions of (a)  $\mu_s$ , (b)  $g_{eff}$ , and (c)  $\Delta n$  for cartilage with intact surface, mild damaged surface, raised surface, and fibrillation lesions, respectively.

the cartilage with intact surface were below  $3 \times 10^{-4}$ , whereas  $\Delta n$  was above  $3 \times 10^{-4}$  in approximately 50% of cartilage with fibrillation, 71% of cartilage with raised surface, and 85% of cartilage with mild damaged surface (Fig. 6(c)). Besides, the cartilage with a mild damaged surface had a wide distribution of  $\Delta n$  that may be due to both collagen thickening and thinning in different areas. The minimum and maximum measured values of  $\Delta n$  in this type of cartilage were  $2.32 \times 10^{-4}$  and  $1.29 \times 10^{-3}$ , respectively.

Our interest in optical characteristics from the medical viewpoint stems from the fact that several changes may occur in a tissue's fine structure and delicate chemical or molecular composition significantly prior to the development of morphological changes in a clinical disease [14–16]. Therefore, accurate knowledge of the optical properties may be helpful for the optimal use of light to determine whether a tissue is normal or diseased [17, 18].

## 5. CONCLUSION

In conclusion, the present study proposes the use of PS-OCT as a noninvasive method to simultaneously evaluate the morphology and quantitative optical properties of articular cartilages. Our preliminary results present that not only subsurface morphological changes include fibrillation, defects, and collagen thickening or thinning but also apparent variation in scattering and birefringence properties, which

may be the early signs of cartilage degeneration, were both found in three types of diseased cartilages. In the future, multinomial logistic regressions can be used to generate a predictive model based on a linear combination of weights of these extracted optical properties. However, an analysis of data using a much larger set of specimens will be required for accurate assessment of the quantitative PS-OCT method in disease grading. Moreover, the use of a longer central wavelength is required so that the cartilage/bone interface is better defined. Hopefully, this study will contribute to develop a quantitative diagnosis method using PS-OCT in arthritis research.

## REFERENCES

1. Chan, W. P., P. Lang, M. P. Stevens, M. S. Sack, E. W. Stoller, C. Basch, and H. K. Genant, "Osteoarthritis of the knee: comparison of radiography, CT, and MR imaging to assess extent and severity," *AJR Am. J. Roentgenol.*, Vol. 157, 799–806, 1991.
2. Huang, D., E. A. Swanson, C. P. Lin, J. S. Schuman, W. G. Stinson, W. Chang, M. R. Hee, T. Flotte, K. Gregory, C. A. Pufialito, and J. G. Fujimoto, "Optical coherence tomography," *Science*, Vol. 254, 1178–1181, 1991.
3. Li, X., S. Martin, C. Pitris, R. Ghanta, D. L. Stamper, M. Harman, J. G. Fujimoto, and M. E. Brezinski, "High-resolution optical coherence tomographic imaging of osteoarthritic cartilage during open knee surgery," *Arthritis Res. Ther.*, Vol. 7, R318–R323, 2005.
4. Adams, Jr., S. B., P. R. Herz, D. L. Stamper, M. J. Roberts, S. Bourquin, N. A. Patel, K. Schneider, S. D. Martin, S. Shortkroff, J. G. Fujimoto, and M. E. Brezinski, "High-resolution imaging of progressive articular cartilage degeneration," *J. Orthop. Res.*, Vol. 24, 708–715, 2006.
5. Herrmann, J. M., C. Pitris, B. E. Bouma, S. A. Boppart, C. A. Jesser, D. L. Stamper, J. G. Fujimoto, and M. E. Brezinski, "High-resolution imaging of normal and osteoarthritic cartilage with optical coherence tomography," *J. Rheumatol.*, Vol. 26, 627–635, 1999.
6. Chu, C. R., D. Lin, J. L. Geisler, C. T. Chu, F. H. Fu, and Y. Pan, "Arthroscopic microscopy of articular cartilage using optical coherence tomography," *The American Journal of Sports Medicine*, Vol. 32, 699–709, 2004.
7. Hee, M. R., D. Huang, E. A. Swanson, and J. G. Fujimoto, "Polarization sensitive low coherence reflectometer for birefringence

- characterization and ranging,” *J. Opt. Soc. Am. B*, Vol. 9, 903–908, 1992.
8. Drexler, W., D. Stamper, C. Jesser, X. Li, C. Pitris, K. Saunders, S. Martin, M. B. Lodge, J. G. Fujimoto, and M. E. Brezinski, “Correlation of collagen organization with polarization sensitive imaging of in vitro cartilage: Implications for osteoarthritis,” *J. Rheumatol.*, Vol. 28, 1311–1318, 2001.
  9. Ugryumova, N., D. P. Attenburrow, C. P. Winlove, and S. J. Matcher, “The collagen structure of equine articular cartilage, characterized using polarization-sensitive optical coherence tomography,” *J. Phys. D: Appl. Phys.*, Vol. 38, 2612–2619, 2005.
  10. Xie, T., S. Guo, J. Zhang, Z. Chen, and G. M. Peavy, “Use of polarization-sensitive optical coherence tomography to determine the directional polarization sensitivity of articular cartilage and meniscus,” *J. Biomed. Opt.*, Vol. 11, 064001~1–064001~8, 2006.
  11. Kuo, W. C., N. K. Chou, C. Chou, C. M. Lai, H. J. Huang, and J. J. Shyu, “Polarization-sensitive optical coherence tomography for imaging human atherosclerosis,” *Appl. Opt.*, Vol. 46, 2520–2527, 2007.
  12. Thrane, L., H. T. Yura, and P. E. Andersen, “Analysis of optical coherence tomography systems based on the extended Huygens-Fresnel principle,” *J. Opt. Soc. Am. A*, Vol. 17, 484–490, 2000.
  13. Clark, J. M., “The organization of collagen fibrils in the superficial zones of articular cartilage,” *J. Anat.*, Vol. 171, 117–130, 1990.
  14. Hayasaki, Y., “Holographic femtosecond laser processing and three-dimensional recording in biological tissues,” *Progress In Electromagnetics Research Letters*, Vol. 2, 115–123, 2008.
  15. Mauriello, P. and D. Patella, “Resistivity tensor probability tomography,” *Progress In Electromagnetics Research B*, Vol. 8, 129–146, 2008.
  16. Zainud-Deen, S. H., W. M. Hassen, E. M. Ali, and K. H. Awadalla, “Breast cancer detection using a hybrid finite difference frequency domain and particle swarm optimization techniques,” *Progress In Electromagnetics Research B*, Vol. 3, 35–46, 2008.
  17. Yan, L., K. Huang, and C. Liu, “A noninvasive method for determining dielectric properties of layered tissues on human back,” *Journal of Electromagnetic Waves and Applications*, Vol. 21, No. 13, 1829–1843, 2007.
  18. Valagiannopoulos, C. A., “On measuring the permittivity tensor of an anisotropic material from the transmission coefficients,” *Progress In Electromagnetics Research B*, Vol. 9, 105–116, 2008.